The following publication Alam, M., Ahmed, G., Ling, Y. T., & Zheng, Y. P. (2018). Measurement of neurovascular coupling in human motor cortex using simultaneous transcranial Doppler and electroencephalography. Physiological Measurement, 39(6), 065005 is available at https://doi.org/10.1088/1361-6579/aac812

Measurement of neurovascular coupling in human motor cortex using simultaneous transcranial Doppler (TCD) and electroencephalography (EEG)

Monzurul Alam[1,*], Ghazanfar Ahmed[1,*], Yan To Ling[1] and Yong-Ping Zheng[1,†]

[1]Department of Biomedical Engineering, The Hong Kong Polytechnic University, Hong Kong

[*]Authors contributed equally

[†]Corresponding author: yongping.zheng@polyu.edu.hk

Abstract:

Objective: Event-related desynchronization (ERD) is a relative power decrease of electroencephalogram (EEG) signals in a specific frequency band during physical motor execution~~;~~, while transcranial Doppler (TCD) measures cerebral blood flow velocity. The objective of this study was to investigate the neurovascular coupling in the motor cortex by using an integrated EEG and TCD system, and to find any difference in hemodynamic responses in healthy young male and female ~~young~~ adults.

Approach: 30 healthy volunteers, aged ~~between~~ 20-30 years were recruited for this study. The subjects were asked to perform a motor task for the duration of a provided visual cue ~~provided~~. Simultaneous EEG and TCD recording was carried out using a new integrated system to detect the ERD arising from the EEG signals, and to measure the mean blood flow velocity~~ies~~ of the left and right middle cerebral arteries from bilateral TCD signals.

Main Results: The r~~R~~esults showed a significant decrease in EEG power in *mu* band (7.5-12.5 Hz) during the motor task compared to the resting phase. It showed significant increase in desynchronization on the contralateral side of the motor task compared to the ipsilateral side. Mean blood flow velocity during the task phase was significantly higher in comparison with the resting phase at the contralateral side. The results also showed a significantly higher increase in the percentage of mean blood flow velocity in the contralateral side of motor task compared to the ipsilateral side. However, no significant difference in desynchronization, or change of mean blood flow velocity was found between males and females.

Significance: A c~~C~~ombined TCD-EEG system successfully detects ERD and blood flow velocity ~~of~~ in cerebral arteries, and can be used as a useful tool to study neurovascular coupling in the brain. There is no significant difference in the hemodynamic responses in healthy young males and females.

1. Introduction:

The h~~H~~uman brain is one of the most metabolically active organs in the body. Although it accounts for only about 2% of ~~the ~~total body weight, it uses roughly 20% of the oxygen of the blood for normal function (Cipolla 2009;~~,~~ Phillips et al 2016). The neurons synthesize adenosine triphosphate (ATP) almost exclusively via glucose and oxygen reaction. Since the brain virtually has no reserved glucose, the blood flow regulation to the brain is tightly maintained (Phillips et al. 2016~~,~~; Zauner & Muizelaar 1997). **Figure 1** shows the vascular architecture of the brain.

Neurovascular coupling modulates the blood flow locally according to the metabolic needs of the regions based on neuronal activity. T~~A t~~ranscranial Doppler (TCD) uses Doppler shifts of ultrasound signals to detect the blood flow velocity in the major brain arteries. TCD provides ~~an~~ inexpensive real-time cerebral artery blood flow measurement. The Doppler shift is directly proportional to the speed of the red blood cells (RBCs) in the blood vessels as blood flow is mostly laminar in arteries. The obtained signal is a spectrum of Doppler shifts formed from different velocities of RBCs. Spectral analysis is then used to obtain different parameters such as blood flow velocity, peak systolic velocity, end diastolic velocity, systolic upstroke (a.k.a. acceleration time), pulsa~~i~~t~~a~~ility index and time averaged mean maximum velocity (Maggio et al. 2013~~,~~; Naqvi et al. 2013~~,~~; Purkayastha & Sorond 2012~~,~~; Yao et al. 2015). Since TCD can provide blood flow velocity changes, it has been used to study the neurovascular coupling effects of different stimuli~~us~~. It ~~has been~~was used to study the interplay of cerebral autoregulation and neurovascular coupling in different orthostatic conditions by Azevedo et al. (2007). In the study, it was found that ~~an ~~intact cerebral autoregulation compensates for blood flow changes ~~in ~~under different orthostatic conditions and allows independent regulation of neurovascular coupling based on the metabolic needs of neural activation. TCD has also been used to show changes in perfusion based on partial pressure of carbon dioxide ($PaCO_2$) changes in blood by measuring blood flow at MCA, PCA, ICA and vertebral artery (VA) (Willie et al. 2012,~~ Willie et al~~ 2014). In addition, neurovascular coupling in motor cortex based on motor stimulus has also been studied using TCD (Azevedo et al. 2007;~~,~~ Conrad & Klingelhöfer 1989~~,~~; Rosengarten et al. 2003~~,~~; Rosengarten & Kaps 2010).

As TCD can provide only information regarding the blood flow changes by measuring blood flow velocity, another measuring tool must be used simultaneously to monitor neuronal activation states. An electroencephalography (EEG) system can detect electrical activities of synchronous firing of neurons by measuring the potentials at the scalp. These signals are then amplified and processed to display information regarding neuronal activation. The EEG waveform recorded from the scalp is quasi-periodic, and for studying they are classified into different frequency bands such as *alpha* (8-15 Hz), *beta* (14-30 Hz), *gamma* (30-70 Hz), *mu* band (7.5-12.5 Hz) etc. (Alam et al. 2016~~,~~; Buzsáki et al. 2012). Different characteristics or changes in the waveforms are linked to different activities; for example, event-related desynchronization (ERD) or event-related synchronization (ERS) in *mu* band represents motor imagery or motor execution (Schomer & da Silva 2012).

A combined TCD and EEG approach has previously been suggested and used to study human visual cortex (Rosengarten & Kaps 2010). A combined TCD-EEG approach ha~~d~~s also been used to study the neurovascular coupling in epilepsy patients (Yao et al. 2015) and for studying cerebral hemodynamics in sleep-~~–~~deprived healthy children (Peng et al. 2016). However, very little study has been reported on the neurovascular coupling responses in major arteries of the Circle of Willis that supplies blood to the motor cortex. No significant gender difference has been shown in previous TCD studies for cognitive activation (Stroobant & Vingerhoets 2000). However, in a recent fMRI study of cognitive inhibition, differences in blood flow were found between males and females (Li et al. 2009). In the current study, we investigated the neurovascular coupling in the motor cortex by using a combined EEG-TCD system; and aimed to find any difference in hemodynamic response between males and females aged ~~between~~ 20-30 years.

2. Methods~~:~~

2.1. Integrated TCD-EEG system

For measuring the neurovascular coupling in the motor cortex, a combined TCD-EEG machine (NSD-7100, Neuro Monitor System) developed by Shenzhen Delica Medical Equipment Co. Ltd., was used. A sketch of the system and its photo is shown in **Figure 2**. TCD and EEG parameters are adjusted through the provided software interface. It also allows recording of the data, which can later be played back and exported to a text file for further processing.

2.2. Flowmeter development

TCD provides the blood flow velocity as a reference of blood flow rate to an area of the brain. So, ideally, the cerebral blood flow velocity should increase linearly with increase in blood flow rate, given that other factors remain constant. Hence, for bench testing the brain blood vessel, there was a need ~~o~~for a flowmeter to measure the changing flow rate of blood. For our study, a custom flowmeter was designed and developed with a data logging facility. An overview of the flowmeter is shown in **Figure 3**. For the flowmeter hardware, a load cell (TAL 220, HT Sensor Technology Co. ~~l~~Ltd., China) with good linearity and sensitivity was utilized. The load cell was interfaced with an interface board (HX711, Sparkfun electronics, USA). The board has a 24-~~–~~bit ADC with adjustable gain. The board was connected to a microcontroller (Arduino Uno, Italy). The digitized voltage representing the load value was stored ~~into~~ on a computer via the microcontroller serial interface.

A c~~C~~ustom computer program was designed to operate the flowmeter and store the readings ~~into~~ as a text file. Once the flow stopped, the microcontroller processed the acquired data. The signal was filtered and averaged to remove noise. As flow rate is the change in volume per unit time, the instantaneous flow rate was calculated by the following equation:

$$Flow\ rate = (V2 - V1)/(T2 - T1)$$

w~~W~~here V1 represents the volume of the fluid at time T1,~~;~~ and V2 is the volume of the fluid at time T2. Only stable flow rate readings in the middle of the experiment were recorded to find the mean value of the flow rate.

2.3. Human experiment

All the experiments were conducted in accordance with the ethical standards. All the subjects had signed informed consents before participating in the study. Ethical approval was obtained from the Ethics Sub-committee of The Hong Kong Polytechnic University (Reference No. HSEARS20170312002). The goal of the human study was to measure neurovascular coupling in the motor region of the brain using a combined TCD-EEG system, and to find any difference between males and females. A total of 30 subjects were recruited for this experiment, 16 males and 14 females, all aged ~~between~~ 20-30 years. All subjects had a temporal window on both sides of their head. Most of the subjects were right-handed. Data for two subjects (1 male and 1 female) were excluded from the study as we found TCD signals were un-retrievable due to noise. The subjects were grouped based on gender~~s~~ for the gender study.

Neurovascular coupling is the change in blood flow to a region of ~~a~~ the brain based on metabolic demand created by activation of local neurons. To measure neurovascular coupling, we needed to simultaneously record EEG activity and blood flow velocity in the particular region of the brain during rest and during particular motor tasks. The EEG signal can be classified into different frequency bands, where each band shows a specific trait based on the cognitive state of the person. In the motor cortex region, event-~~–~~related desynchronization (ERD)/event-~~–~~related synchronization (ERS) was observed in the *mu* frequency band (8-13 Hz). ERD/ERS is simply a decrease/increase in power of *mu* band during motor imagery and motor execution. ERD/ERS is prominent in the C3 and C4 region of the international 10-20 EEG system (Pfurtscheller & Lopes da Silva 1999). So, in our experiment, we recorded EEG signals from channel C3 and C4. A r~~R~~eference signal was calculated by averaging the A1 and A2 (place on the right and left ear lobe). The ground channel was connected to the Cz location.

Blood supply to the motor cortex comes from the MCA and ACA; while MCA supplies blood to the region responsible for the upper limbs, ACA supplies the region responsible for the lower limbs (Ugur et al. 2005). As our task involved fist forming, simultaneous recording of the right and left MCA was done using TCD probes 1 and 2 through the temporal windows. An adjustable headframe was used to hold the two TCD probes in position. TCD probes were placed and fixed with a sufficient amount of gel. The probes were adjusted to obtained good intensity of TCD signal. The TCD parameters used for each subject are shown in the **Supplementary T~~t~~able 1**. The skin of the head of the subject was prepared with EEG gel and electrodes were attached to ensure that the impedance of each of the connected electrodes was below 25 kΩ. EEG signal was band-pass filtered (0.53-30 Hz) and digitized at 1 kHz. After system setup, eye blink and teeth crunch tests were carried out to check EEG functionality. In our experiment, the subjects were asked to focus and form a fist and release with his/her right hand, repeatedly, in response to a signal given by a light emitting diode (LED). The LED starteds from the OFF state for 30 secs to relax for EEG signal stabilization. Then the LED turneds ON for 30 seconds during which the subject performsed the task. The LED then turnsed OFF for 30 seconds during which the subject relaxeds, thus completing one cycle of the experiment task. Each subject carried out five5 cycles of the task, during which the EEG and TCD data was were recorded. The subjects were instructed to do perform fist forming and release for a random number of times. They were also instructed to blink as little as possible, relax and not to move their body during the experiment to minimize the noise.

2.4. Data analysis and statistics

The output file from the system containeds both TCD and EEG data. The TCD data contained the envelope value of the TCD waveform. The EEG signal containeds eye blink noise, 50 Hz noise and its harmonics, as well as some subject- movement-related noises. Hence, we needed further filtering of the EEG signal in order to extract ERD/ERS data from the specific frequency band. A custom script was written in MATLAB (MathWorks Inc., USA) for signal processing of all the subjects' EEG and TCD data. The data were then processed and output of as ERD/ERS percentage and change in mean blood flow velocity percentage for C3, C4, left MCA (LMCA) and right MCA (RMCA). To calculate the power in of each frequency components of the signal, short-time Fourier transform (STFT) was performed. The data wereas then used to plot the time frequency analysis map for both rest and task phases. Cumulative powers for 30 seconds, for each frequency, for both rest and task phases were then calculated and plotted. The ERD/ERS was then measured by calculating the area under the curve for cumulative power curves. The equation for calculating ERD/ERS is provided below:

% ERD or ERS = (cumulative power during rest - cumulative power during task)/(cumulative power during rest) ×100

This was done for each of the cycles for every subject. Thus, we got 5obtained five ERD/ERS per channel, per subject,; which were then used to calculate the mean and standard deviation of ERD/ERS of each channel for each subject. The result for each channel was recorded in a table and was used for statistical analysis.

From the text file exported from the TCD-EEG system, we got obtained the envelope value of the TCD signal for the LMCA and RMCA. The data was were first epoched based on the start and stop peak. After epoching the data was they were preprocessed visually for any artifacts or zero values;, andwhich were removed. The maximum systolic blood flow velocity and its index for each heartbeat were found using the custom script written in MATLAB (MathWorks Inc., USA). The prominence of the peak was set to be half of the difference between the maximum and minimum value of the signal, with a minimum peak distance of 400 milliseconds (as it was highly unlikely for the heartbeat rate to cross exceed 160 bpm during testing). The data was were then inversed and the same method was used to find the end diastolic velocity and its index. The mean flow velocity of each heartbeat was then calculated using the equation below:

$$Mean\ Flow\ Velocity = (Peak\ Systolic\ Velocity + (2 \times End\ Diastolic\ Velocity))/3$$

The mean flow velocity was then calculated for the whole phase. The process was repeated for all rest and task phases for both right and left MCA of each subject. The data of each MCA for each subject ~~was~~ were recorded for statistical analysis.

Differences between groups were considered statistically significant at P<0.05. All the statistical analyses were performed using Prism (GraphPad Software Inc., USA).

3. Results~~:~~

3.1. Bench test results of TCD

An initial bench test of the TCD system was carried out to find any offset and any difference in linearity between the two probes. The bench test was carried out using a silicone pipe dipped into a container filled with a mixture of water and oat bran powder. The mixture has finely milled colloidal particles of oat bran that reflect~~s~~ ultrasound and creates a Doppler shift similar to blood. An electric water pump was used to flow the mixture at a constant rate through the tube shown in **Figure 3B**. One TCD probe was held at an approximately 30-degree angle to the silicone pipe at a fixed depth. It was adjusted to achieve the highest possible mean flow velocity reading on the TCD monitor, and the value was recorded. Then another TCD probe was used in place of the first TCD probe in a similar manner to achieve the highest possible mean flow velocity, and the value was recorded. After this the output flow pipe was moved from the reservoir to the flow meter and the real flow rate was recorded from the flowmeter system. The process was repeated with a change in input voltage to the pump and hence a change in the flow rate. Mean flow velocity for each probe and the flow rate were recorded and ~~were~~ tabulated for different input voltage to the pump as shown in Table 1. The volumetric flow rate is given by the equation below:

$$Volumetric\ Flow\ Rate = Cross\text{-}sectional\ Area \times Flow\ Velocity$$

From Table 1 we can see that the flow velocity was directly proportional to the flow rate for both probes as the proportionality constant was fairly stable. Hence, we found that the flow velocity~~ies~~ ~~were~~ was linear and there was no significant difference (P = 0.4) between the linearity of the probes. Also, there was no significant difference (P = 0.422) between the mean flow velocity values of the two probes at ~~a~~ the same flow rate~~.~~, ~~T~~thus showing that there was no baseline offset between the two probes.

3.2. TCD-EEG results on human subjects

Our collected EEG signal contained ambient electromagnetic noise. Hence, we ran a number of signal processing steps on these data to clear the noise. **Figure 4** shows the raw and filtered EEG data of one representative subject. Low- and high-~~-~~frequency noises including 50 Hz line noise and its harmonic frequencies were filtered out from the EEG signal as shown in **Figure 4A**. **Figure 4B** shows the time frequency graphs and cumulative power values of EEG signals. It can be observed from the graphs that there was higher power in the resting phase compared to the task phase. It is also apparent that the desynchronization occurred from 10 Hz onwards. **Figure 5** shows simultaneous recording of ~~-~~EEG and TCD signals during ~~a~~ the task phase and its following resting phase of a subject. Comparing the two phases, apparently higher power in the C3 EEG signal is accompanied by lower cyclic mean blood flow velocity at LMCA in the resting phase.

The values of area under the power curve in the *mu* band during the resting phase and task phase of C3 and C4,~~;~~ and the values of average mean blood flow during the resting phase and task phase were compared for statistical differences using a paired t-test for each subject. Based on the values and results obtained, bar plots for C3 and C4,~~;~~ and box-and-whisker plots for LMCA and RMCA were plotted for each subject. **Figure 6** shows a representative result from one subject.

Table 2 shows the overall results ~~from~~ for all the human subjects. ~~M~~The mean value was obtained by averaging the area under the curve of power-frequency diagram of the phases over trials. The ERD/ERS was calculated using the following equation:

ERD or ERS % = (Average Resting Phase Power - Average Task Phase Power)/(Average Resting Phase Power)×100

A similar equation was used to calculate the percentage increase or decrease in mean blood flow velocity. Hence, a positive value of ERD/ERS indicates desynchronization whereas a positive value of percentage changes in mean flow velocity indicates decreased velocity and vice versa.

The ERD/ERS values of C3 and C4, and percentage change in mean blood flow velocity in LMCA and RMCA were also compared for any statistical difference. **Figure 7** shows the comparison of C3 vs. C4 and LMCA vs. RMCA of one subject. The overall result for all the subjects ~~were~~ was calculated for C3 vs. C4~~,~~ and LMCA vs. RMCA. The values are presented as mean and standard deviation in ~~the~~ Table 3.

From **Table 2**, we can see that 26 out of 28 subjects had significant ERD/ERS in the *mu* band in the C3 region during the motor task. Among these 26 subjects, 25 subjects showed desynchronization and only ~~1~~ one subject ~~showed~~ exhibited synchronization. From the same table, it is observed that for C4 region, 16 out of 28 subjects showed significant ERD/ERS patterns. From these 16 subjects, 11 subjects ~~showed~~ exhibited significant desynchronization whereas ~~5~~ five subjects ~~showed~~ exhibited significant synchronization. The remaining subjects also ~~showed~~ exhibited ERS/ERD, but were not statistically significant. When we compared the ERD/ERS between C3 and C4 for all subjects (**Figure 7A**), we found that there was a significant difference ($P<0.05$) between C3 and C4 ERD/ERS. From this data set we observed that the ERD/ERS wa~~i~~s more prominent in the C3 region compared to C4 region.

Again, from **Table 2**, we found that 27 out of 28 subjects ~~show~~ exhibited a significant difference in mean blood flow velocit~~ies~~y in the LMCA between the resting phase and ~~the~~ task phase. We also observed significant increases in mean blood flow velocit~~ies~~y during the task phase when compared to the resting phase in 26 out of 27 subjects. For RMCA, however, only two~~2~~ out of 28 subjects

~~showed~~ exhibited significant changes in the mean blood flow velocity~~ies~~ between the resting phase and task phase. Both subjects ~~showed~~ exhibited an increase in mean blood flow velocity~~ies~~. From the remaining subjects, ~~7~~ seven subjects exhibited a ~~showed~~ decrease in blood flow velocity~~ies~~ while others exhibited an ~~showed~~ increase in mean blood flow velocity;~~ies,~~ however, none of them ~~was~~ were statistically significant. We further compared the percentage changes in mean blood flow velocity~~ies~~ between LMCA and RMCA for all the subjects. Our results showed that there was a significant difference (P<0.05) in the percentage changes in mean blood flow velocity~~ies~~ between LMCA and RMCA (**Figure 7B**). When compared to RMCA, the LMCA showed a higher percentage change~~s~~ in blood flow velocity~~ies~~ between the resting phase and task phase.

The C3, C4, LMCA and RMCA data were further separated based on gender for comparison. **Figure 8** shows the overall result for gender comparison. The mean and standard values for the gender-based study are given in ~~the~~ Table 4. From the gender dependence study, we observed no significant difference in desynchronization, or change of mean blood flow velocity between young males and females (**Figure 8**). Both ipsilateral and contralateral sides of the motor activation task showed no significant difference. However, we found desynchronization and a percentage change in mean blood flow velocity in the C4 region and RMCA was higher in females than in males. But these differences were not statistically significant.

4. Discussion~~:~~

The EEG results match ~~with~~ th~~at~~ose reported in previous studies (Bai et al. 2005), showing contralateral ERD/ERS during motor actions. However, in our study we found that some subjects exhibited event~~-~~-related synchronization rather than desynchronization. This may be because ERD patterns occur~~s~~ at different frequency ranges for every individual. But most commonly ~~it is~~they are exhibited in the *mu* band. Furthermore, since we calculated the area under the curve for the whole *mu* band, if desynchronization occurred at a smaller frequency range than synchronization in the *mu* band, the overall result would show synchronization even if there was a small desynchronization. This may be the reason why we saw a higher number of synchronization values in the C4 region. All our results showed more prominent desynchronization on the contralateral side of motor activation in agreement with the current knowledge on ERD/ERS (Bai et al. 2005). Thus our integrated system shows the capability of detecting ERD/ERS from the EEG data.

The TCD result is in ~~the~~ agreement with the pattern of TCD blood flow lateralization in the contralateral hemisphere observed by others (Silvestrini et al. 1998). Thus, the integrated system also ~~showed~~ demonstrated its capability ~~of~~ to detect~~ing~~ changes in blood flow velocity~~ies~~ from the TCD data. However, blood pressure is also known to change during ~~the~~ hand grip tasks (Kwan et al. 2004). But, as we are interested in ~~the~~ brain activity and ~~it's~~ the blood flow in different brain regions during ~~the~~ motor tasks, we di~~ha~~d not monitor~~ed the~~ blood pressure changes in our study. Nonetheless, we identify this as a limitation of our current study and will measure the blood pressure in our future studies on neurological patients using our integrated system.

Several previous studies have combined ~~the~~ EEG and TCD monitoring to study hemispheric dominance (Szirmai et al. 2005), carotid endarterectomy monitoring (Jansen et al. 1993), cerebral hemodynamics (Niehaus et al. 2000), and anesthetic response (Kochs et al. 1991). Hence, there is a need for simultaneous recording of EEG and TCD signals. However, to the best of our knowledge, the system presented in our paper is the first complete system which combines the two imaging and electrophysiological modalities into one machine. ~~In a~~A recent study on healthy subjects performing a hand grip task showed significant correlations between blood oxygen level-dependent (BOLD) fMRI signal and EEG rhythms modulations, identifying task-related, well localized activated volumes (Sclocco et al. 2014). From the literature we also found that no significant gender difference has been shown in previous TCD studies for cognitive activation (Stroobant & Vingerhoets 2000). However, in another fMRI study of cognitive inhibition, differences in blood flow were found between males and females (Li et al. 2009). Since there are potentially contradicting results in the literature, we thought that it ~~is~~ would be worthwhile to reinvestigate the gender difference in neurovascular coupling.

One of the limitations of the current study was the sample size. For the comparison between ERD/ERS in C3 and C4, and percentage change in blood flow velocity in LMCA and RMCA, we recruited 28 subjects. However, for the gender dependence experiment, the samples from male and female populations were 15 and 13, respectively. This may have introduced error in the results of the experiment. Another major limitation of the study was noise rejection. We chose to prevent noise by asking the subjects not to blink or move much. However, the subjects had to blink due to natural urge. This was one of the sources of noise~~s;~~, which was later manually removed. This method may have compromised the quality of the data. Advanced signal processing methods such as ICA for noise removal from both EEG and TCD should be used in future studies. To study the neurovascular coupling in the motor cortex, the whole motor cortex should have been studied. Instead, we designed our experiment to focus on the left hemisphere by fixing the motor task to the right hand only. Furthermore, there were certain parameters not studied such as time taken for maximum vascular reaction to occur, gain parameter, etc.

5. Conclusion~~:~~

The c~~C~~urrent study utilized~~s~~ a combined TCD and EEG system to study the neurovascular coupling in the motor cortex. The results showed a significant decrease in EEG power in *mu* band during motor tasks at the contralateral side compared to the resting phase. Also, there was a significant increase in desynchronization at the contralateral side during the motor task. TCD results showed a significant increase in mean blood flow velocity during the task phase compared to the resting phase at the contralateral side. The results also showed a significant increase in the percentage of mean blood flow velocity at the contralateral side during the motor task. From these results we can conclude that there was higher neurovascular coupling on the contralateral side of the brain during the motor task because both ERD and the percentage increase in mean blood flow velocity were higher. No significant differences in desynchronization or mean blood flow velocity were, however, observed between young males and females.

Since the results match ~~with~~ th~~at~~ose of previous literature, we may conclude that the combined TCD and EEG system is an effective tool for studying neurovascular coupling. The dual-modality system saves users ~~from~~ the trouble of synchronization of multiple systems, making it more convenient for clinical research.

In the current study, we only recruited a limited number of healthy subjects restricted to a certain age group. Recent studies suggest that ~~the~~ changes in neurovascular coupling play~~s~~ an important role in different disease conditions such as stroke and dementia, etc. (Girouard & Iadecola 2006). Hence, future experiments should include more subjects with different populations to study and compare the changes in neurovascular coupling in different pathologies. Also, better noise rejection techniques and a more accurate synchronization system should be used. Furthermore, while analyzing the EEG signal, only the desynchronizing zone should be used in calculations, as using the whole *mu* band may ~~provide~~ generate erroneous results. Future study design should include the whole motor cortex and neurovascular coupling in other arteries such as ACA, which also supplies blood to some regions of the motor cortex.

6. Acknowledgements:

This research study was supported by the Hong Kong Polytechnic University (G-YBFV, G-YBRN, H-ZG4W). The authors would like to thank all the participants for volunteering ~~to~~ for the study and Ms. Tian Ge for her help i~~o~~n writing computer codes for data analysis.

References:

Alam M, Rodrigues W, Pham BN, Thakor NV. 2016. Brain-machine interface facilitated neurorehabilitation via spinal stimulation after spinal cord injury: Recent progress and future perspectives. *Brain Research* 1646: 25-33

Azevedo E, Rosengarten B, Santos R, Freitas J, Kaps M. 2007. Interplay of cerebral autoregulation and neurovascular coupling evaluated by functional TCD in different orthostatic conditions. *Journal of Neurology* 254: 236-41

Bai O, Mari Z, Vorbach S, Hallett M. 2005. Asymmetric spatiotemporal patterns of event-related desynchronization preceding voluntary sequential finger movements: a high-resolution EEG study. *Clinical Neurophysiology* 116: 1213-21

Buzsáki G, Anastassiou CA, Koch C. 2012. The origin of extracellular fields and currents — EEG, ECoG, LFP and spikes. *Nature Reviews Neuroscience* 13: 407

Cipolla MJ. 2009. *The Cerebral Circulation*. Morgan & Claypool Publishers.

Conrad B, Klingelhöfer J. 1989. Dynamics of regional cerebral blood flow for various visual stimuli. *Experimental Brain Research* 77: 437-41

Girouard H, Iadecola C. 2006. Neurovascular coupling in the normal brain and in hypertension, stroke, and Alzheimer disease. *Journal of Applied Physiology* 100: 328-35

Jansen C, Moll FL, Vermeulen FEE, van Haelst JMPI, Ackerstaff RGA. 1993. Continuous transcranial Doppler ultrasonography and electroencephalography during carotid endarterectomy: A multimodal monitoring system to detect intraoperative ischemia. *Annals of Vascular Surgery* 7: 95-101

Kochs E, Werner C, Hoftman WE, Möllenberg O, Schulte am Esch J. 1991. Concurrent increases in brain electrical activity and intracranial blood flow velocity during low-dose ketamine anaesthesia. *Canadian Journal of Anaesthesia* 38: 826-30

Kwan J, Lunt M, Jenkinson D. 2004. *Assessing dynamic cerebral autoregulation after stroke using a novel technique of combining transcranial Doppler ultrasonography and rhythmic handgrip*. 3-8 pp.

Li C-sR, Zhang S, Duann J-R, Yan P, Sinha R, Mazure CM. 2009. Gender Differences in Cognitive Control: an Extended Investigation of the Stop Signal Task. *Brain Imaging and Behavior* 3: 262-76

Maggio P, Salinet ASM, Panerai RB, Robinson TG. 2013. Does hypercapnia-induced impairment of cerebral autoregulation affect neurovascular coupling? A functional TCD study. *Journal of Applied Physiology* 115: 491-97

Naqvi J, Yap KH, Ahmad G, Ghosh J. 2013. Transcranial Doppler Ultrasound: A Review of the Physical Principles and Major Applications in Critical Care. *International Journal of Vascular Medicine* 2013: 629378

Niehaus L, Wieshmann UC, Meyer BU. 2000. Changes in Cerebral Hemodynamics during Simple Partial Motor Seizures. *European Neurology* 44: 8-11

Peng B, Li J, Wang J, Liang X, Zheng Z, Mai J. 2016. Changes in cerebral hemodynamics during a sleep-deprived video-electroencephalogram in healthy children. *Physiological Measurement* 37: 981

Pfurtscheller G, Lopes da Silva FH. 1999. Event-related EEG/MEG synchronization and desynchronization: basic principles. *Clinical Neurophysiology* 110: 1842-57

Phillips AA, Chan FHN, Zheng MMZ, Krassioukov AV, Ainslie PN. 2016. Neurovascular coupling in humans: Physiology, methodological advances and clinical implications. *Journal of Cerebral Blood Flow & Metabolism* 36: 647-64

Purkayastha S, Sorond F. 2012. Transcranial Doppler Ultrasound: Technique and Application. *Seminars in neurology* 32: 411-20

Rosengarten B, Budden C, Osthaus S, Kaps M. 2003. Effect of Heart Rate on Regulative Features of the Cortical Activity-Flow Coupling. *Cerebrovascular Diseases* 16: 47-52

Rosengarten B, Kaps M. 2010. A Simultaneous EEG and Transcranial Doppler Technique to Investigate the Neurovascular Coupling in the Human Visual Cortex. *Cerebrovascular Diseases* 29: 211-16

Schomer DL, da Silva FL. 2012. *Niedermeyer's Electroencephalography: Basic Principles, Clinical Applications, and Related Fields*. Wolters Kluwer Health.

Sclocco R, Tana MG, Visani E, Gilioli I, Panzica F, et al. 2014. EEG-informed fMRI analysis during a hand grip task: estimating the relationship between EEG rhythms and the BOLD signal. *Frontiers in Human Neuroscience* 8: 186

Silvestrini M, Cupini LM, Placidi F, Diomedi M, Bernardi G. 1998. Bilateral Hemispheric Activation in the Early Recovery of Motor Function After Stroke. *Stroke* 29: 1305-10

Smith WS, Johnston SC, Hemphill JC. 2015. Cerebrovascular Diseases In *Harrison's Principles of Internal Medicine, 19e*, ed. D Kasper, A Fauci, S Hauser, D Longo, JL Jameson, J Loscalzo. New York, NY: McGraw-Hill Education

Stroobant N, Vingerhoets G. 2000. Transcranial Doppler Ultrasonography Monitoring of Cerebral Hemodynamics During Performance of Cognitive Tasks: A Review. *Neuropsychology Review* 10: 213-31

Szirmai I, Amrein I, Pálvölgyi L, Debreczeni R, Kamondi A. 2005. Correlation between blood flow velocity in the middle cerebral artery and EEG during cognitive effort. *Cognitive Brain Research* 24: 33-40

Ugur HC, Kahilogullari G, Coscarella E, Unlu A, Tekdemir I, et al. 2005. Arterial vascularization of primary motor cortex (precentral gyrus). *Surgical Neurology* 64: S48-S52

Willie CK, Macleod DB, Shaw AD, Smith KJ, Tzeng YC, et al. 2012. Regional brain blood flow in man during acute changes in arterial blood gases. *The Journal of Physiology* 590: 3261-75

Willie CK, Tzeng Y-C, Fisher JA, Ainslie PN. 2014. Integrative regulation of human brain blood flow. *The Journal of Physiology* 592: 841-59

Yao Y, Lu Q, Jin L-R, Zhou X-Q, Huang Y, Xu W-H. 2015. Real-time TCD-vEEG monitoring for neurovascular coupling in epilepsy. *Seizure* 29: 1-3

Zauner A, Muizelaar JP. 1997. Brain metabolism and cerebral blood flow In *Head Injury: Pathophysiology and Management of Severe Closed Injury*, ed. P Reilly, R Bullock, pp. 89-99. London: Chapman & Hall

Figure and Table legends:

Figure 1. Major blood supply to the brain, dictated~~s~~ by the arteries that branch off from the aorta. The i~~I~~nternal carotid artery (ICA) branch ~~to~~ forms two major cerebral arteries: anterior cerebral artery (ACA) and the middle cerebral artery (MCA). Posterior Cerebral artery: PCA. Modified from (Smith et al. 2015).

Figure 2. (A) Sketch of the combined TCD-EEG neuromonitoring system. (B) EEG terminal, TCD headframe, keyboard controller hardware and software interface of the neuromonitoring system.

Figure 3. (A) Block diagram and hardware circuit of the flowmeter. (B) Illustration of the experimental setup for the bench test. The silicon pipe was passed through the water container. Ultrasound probes were held with the tip dipped under water and the flow through the pipe was measured using both probes.

Figure 4. (A) Five seconds of raw EEG signal before and after filtering and noise cancel~~l~~ation (left column) and their corresponding welch power spectral density estimation (right column). Low- and high -frequency noises including the 50 Hz line noise and it~~'~~s harmonic frequencies were filtered out. (B) The f~~F~~irst two rows show short-time Fourier transformation (STFT) of filtered EEG signals during the task phase and resting phase. The last row shows the cumulative power value for each frequency during the resting and task phases which indicates that the desynchronization occurred from 10 Hz onwards.

Figure 5. Short-time Fourier transformation (STFT) of filtered EEG signals from C3 during the task phase (top) and resting phase (middle), with the cyclic mean blood flow velocity at LMCA (bottom) during the task phase (red) and resting phase (blue) in the same time scale.

Figure 6. (A) Area under the power curve in *mu* band for C3 and C4 EEG channels during the resting and task phases. (B) Mean blood flow velocity for LMCA and RMCA during the resting and task phases. **: significantly different at $P<0.05$.

Figure 7. (A) Comparison of C3 and C4 ERD/ERS values. (B) Comparison of LMCA and RMCA percentage change in mean blood flow velocity. **: significantly different at $P<0.05$; and ****: significantly different at $P<0.001$.

Figure 8. (A) C3 and C4 for comparison between males and females. (B) LMCA and RMCA for comparison between males and females.

Table 1. The table shows the input voltage of the pump, mean flow values obtained from both probes and the real flow rate obtained from the flowmeter.

Table 2. The table shows the average area under the power frequency curve during the resting and task phases of C3 and C4. It also shows the average of mean flow velocit~~ies~~y of LMCA and RMCA. The resting and task phase values for each trial were statistically compared to find any significant difference. Significantly different values are highlighted by highlighting the *P*-values in blue ($P<0.05$).

Table 3. Table showing the mean and standard deviation of each channel and probe~~.~~

Table 4. Table showing the mean and standard deviation of each channel and probe for males and females

Supplementary Table 1. Table showing TCD parameters used for each subject, including depth, gate, gain and amplitude of each channel

Table 1

Pump input voltage (volts)	**Flow rate** (ml/s)	**Mean flow velocity**		**Flow rate / Mean flow velocity**	
		Probe 1 (cm/s)	Probe 2 (cm/s)	Probe 1 (ml/cm)	Probe 2 (ml/cm)
6	17.76	64	65	0.2775	0.2732
9	24.16	87	87	0.2777	0.2777
12	25.80	95	95	0.2716	0.2716

Table 2

S/N	Sex	C3 Channel EEG results				LMCA TCD results				C4 Channel EEG results				RMCA TCD results			
		Area under the power curve				Mean flow velocity				Area under the power curve				Mean flow velocity			
		Rest phase (μW.Hz)	Task phase (μW.Hz)	ERD/ERS (%)	P-value	Rest phase (cm/s)	Task phase (cm/s)	Change in mean flow velocity (%)	P-value	Rest phase (μW.Hz)	Task phase (μW.Hz)	ERD/ERS (%)	P-value	Rest phase (cm/s)	Task phase (cm/s)	Change in mean flow velocity (%)	P-value
1	M	833621.2	474013.5	43.13802	**0.0075**	60.61324	62.39898	-2.94612	**0.0219**	768853.5	488743.1	36.43222	**0.0302**	54.74147	55.36905	-1.14643	0.0516
2	F	2221062	797622	64.08827	**0.0330**	61.24089	64.8619	-5.91273	**0.0066**	2127913	1009526	52.55795	**0.0453**	60.75683	62.58886	-3.01535	0.0797
3	F	501742.9	406631.1	18.95628	**0.0178**	54.00339	55.92354	-3.55563	**0.0254**	616922.1	560139.8	9.204131	**0.0296**	52.60729	53.34918	-1.41025	0.2398
4	M	317111.4	360832.2	-13.7872	0.1024	53.4449	58.31348	-9.10954	**0.0191**	816551	794002.6	2.761412	0.7327	52.86625	56.89169	-7.61439	**0.0044**
5	M	1241320	480645.1	61.27951	**< 0.0001**	57.91985	60.61421	-4.65187	**0.0071**	724528.5	509092.6	29.73463	**0.0167**	62.11139	63.48286	-2.20809	0.0942
6	F	471542.2	300143.8	36.34847	**0.0006**	59.76406	62.05033	-3.8255	**0.0236**	485002.6	278391.7	42.59995	**0.0025**	68.58304	69.16306	-0.84571	0.7489
7	F	1413782	787666.2	44.28657	**0.0132**	79.71424	86.07161	-7.97519	0.6983	937754.6	932287.9	0.582952	**0.0121**	79.01554	80.44445	-1.80839	0.6983
8	M	285366.8	247971.7	13.10423	**0.0422**	65.12522	66.25296	-1.73165	**0.0425**	304674.3	276314.9	9.308116	0.4378	62.50001	63.31917	-1.31066	0.2398
9	M	759061.5	584649.5	22.97733	**0.0323**	43.20728	44.24732	-2.40708	**0.0204**	738241.7	606796.2	17.8052	**0.0979**	45.07904	45.33609	-0.57023	0.7266
10	M	635874.9	477728.8	24.87064	**0.0304**	50.04751	51.39047	-2.68336	**0.0386**	687838.5	1262006	-83.4741	**0.0015**	54.04651	54.90103	-1.58108	0.0912
11	M	3122993	794226.8	74.56841	**0.0021**	45.77975	48.25534	-5.40759	**0.0020**	3010537	2535174	15.79	0.2415	48.6163	46.16458	5.042993	0.1091
12	F	417698.7	238409.9	42.923	**0.0135**	72.54318	74.98261	-3.36272	**0.0043**	443382.2	364864.4	17.70882	0.2663	69.66835	70.6005	-1.33799	0.2704
13	F	324918.8	276989.5	14.75116	**0.0265**	54.87918	57.81239	-5.34485	**0.0061**	407035.9	722069.1	-77.3969	**0.0030**	57.47213	59.31043	-3.19859	**0.0119**
14	F	829839.7	560411.4	32.4675	**0.0013**	61.08392	63.25924	-3.56119	**0.0383**	737476.8	983038.9	-33.2976	0.1777	73.32869	74.90918	-2.15535	0.1986
15	F	956113.8	492031.4	48.53841	**0.0490**	36.38875	37.90859	-4.17668	**0.0250**	935539.9	501162.8	46.43063	0.0527	52.77337	53.52053	-1.41579	0.4539
16	M	385583.2	249680.4	35.24604	**0.0024**	53.44781	59.94919	-12.164	**0.0319**	746545.9	2608255	-249.376	**<0.0001**	54.8809	50.57191	7.85153	0.4237
17	M	442629.1	482450.8	-8.99662	0.3687	55.37261	59.22731	-6.96139	**0.0435**	1333106	1484432	-11.3514	0.7670	62.79601	64.60554	-2.8816	0.3644
18	F	636387.2	513975.5	19.23542	**0.0482**	42.33048	44.18448	-4.37981	**0.0496**	883217.5	592851.9	32.87589	**0.0210**	40.59703	39.57867	2.508457	0.2762
19	F	1759114	753588.7	57.16089	**0.0466**	78.00596	81.03541	-3.88361	**0.0373**	1942535	1075573	44.63048	0.0917	71.95541	73.80359	-2.56851	0.2125
20	F	700779	562403.4	19.74597	**0.0357**	59.19581	62.90497	-6.26591	**0.0065**	803649.8	666643.6	17.048	0.0867	70.1611	72.30929	-3.0618	0.0508
21	F	938719	649050.3	30.85787	**0.0445**	53.77011	55.01905	-2.32273	**0.0088**	932487	704767.4	24.42067	**0.0487**	48.13208	48.54767	-0.86343	0.3842
22	M	695571.4	329074	52.69013	**0.0084**	70.10543	71.58024	-2.10371	**0.0137**	396771.1	1134271	-185.875	**0.0130**	71.7653	71.52152	0.339691	0.8056
23	M	1792763	885890.5	50.5852	**0.0118**	46.90816	48.51118	-3.41736	**0.0225**	1902609	1000375	47.42088	**0.0074**	47.41775	48.16717	-1.58046	0.4843
24	M	370352.1	297486.5	19.67468	**0.0354**	36.93544	36.10587	2.246018	**0.0433**	365162.6	352625.5	3.433272	0.7238	31.9328	30.83026	3.452695	0.1135
25	F	417973.6	538377	-28.8065	**0.0394**	40.65702	42.71012	-5.04982	**0.0126**	356757.2	450702.4	-26.3331	**0.0485**	51.8658	50.40421	2.818016	0.1499
26	M	1403656	820228.3	41.56487	**0.0023**	57.09534	61.2957	-7.35674	**0.0404**	1146966	1790875	-56.1401	0.2273	59.60672	59.55645	0.084334	0.9718
27	M	1499338	372312	75.16824	**0.0288**	58.97941	61.0317	-3.47968	**0.0360**	1173768	836491.7	28.73449	0.1327	58.31743	58.45199	-0.23074	0.8814
28	M	1543925	764473.5	50.48506	**0.0484**	51.55398	54.45837	-5.63368	**0.0434**	842998	730047.4	13.39868	**0.0108**	60.19055	62.058	-3.10256	0.2687

S/N	Sex	C3 Channel EEG results				LMCA TCD results				C4 Channel EEG results				RMCA TCD results			
		Area under the power curve				Mean flow velocity		Change in mean flow velocity (%)		Area under the power curve				Mean flow velocity		Change in mean flow velocity (%)	
		Resting phase (mW.Hz)	Task phase (mW.Hz)	ERD/ERS (%)	P-value	Resting phase (cm/s)	Task phase (cm/s)		P-value	Resting phase (mW.Hz)	Task phase (mW.Hz)	ERD/ERS (%)	P-value	Resting phase (cm/s)	Task phase (cm/s)		P-value
1	M	833.6	474.0	43.14	**0.0075**	60.6	62.4	-2.95	**0.0219**	768.9	488.7	36.43	**0.0302**	54.7	55.4	-1.15	0.0516
2	F	2221.1	797.6	64.09	**0.033**	61.2	64.9	-5.91	**0.0066**	2127.9	1009.5	52.56	**0.0453**	60.8	62.6	-3.02	0.0797
3	F	501.7	406.6	18.96	**0.0178**	54.0	55.9	-3.56	**0.0254**	616.9	560.1	9.20	**0.0296**	52.6	53.3	-1.41	0.2398
4	M	317.1	360.8	-13.79	0.1024	53.4	58.3	-9.11	**0.0191**	816.6	794.0	2.76	0.7327	52.9	56.9	-7.61	**0.0044**
5	M	1241.3	480.6	61.28	**< 0.0001**	57.9	60.6	-4.65	**0.0071**	724.5	509.1	29.73	**0.0167**	62.1	63.5	-2.21	0.0942
6	F	471.5	300.1	36.35	**0.0006**	59.8	62.1	-3.83	**0.0236**	485.0	278.4	42.60	**0.0025**	68.6	69.2	-0.85	0.7489
7	F	1413.8	787.7	44.29	**0.0132**	79.7	86.1	-7.98	0.6983	937.8	932.3	0.58	**0.0121**	79.0	80.4	-1.81	0.6983
8	M	285.4	248.0	13.10	**0.0422**	65.1	66.3	-1.73	**0.0425**	304.7	276.3	9.31	0.4378	62.5	63.3	-1.31	0.2398
9	M	759.1	584.6	22.98	**0.0323**	43.2	44.2	-2.41	**0.0204**	738.2	606.8	17.81	**0.0979**	45.1	45.3	-0.57	0.7266
10	M	635.9	477.7	24.87	**0.0304**	50.0	51.4	-2.68	**0.0386**	687.8	1262.0	-83.47	**0.0015**	54.0	54.9	-1.58	0.0912
11	M	3123.0	794.2	74.57	**0.0021**	45.8	48.3	-5.41	**0.002**	3010.5	2535.2	15.79	0.2415	48.6	46.2	5.04	0.1091
12	F	417.7	238.4	42.92	**0.0135**	72.5	75.0	-3.36	**0.0043**	443.4	364.9	17.71	0.2663	69.7	70.6	-1.34	0.2704
13	F	324.9	277.0	14.75	**0.0265**	54.9	57.8	-5.34	**0.0061**	407.0	722.1	-77.40	**0.003**	57.5	59.3	-3.20	**0.0119**
14	F	829.8	560.4	32.47	**0.0013**	61.1	63.3	-3.56	**0.0383**	737.5	983.0	-33.30	0.1777	73.3	74.9	-2.16	0.1986
15	F	956.1	492.0	48.54	**0.049**	36.4	37.9	-4.18	**0.025**	935.5	501.2	46.43	0.0527	52.8	53.5	-1.42	0.4539
16	M	385.6	249.7	35.25	**0.0024**	53.4	59.9	-12.16	**0.0319**	746.5	2608.3	-249.38	**<0.0001**	54.9	50.6	7.85	0.4237

17	M	442.6	482.5	-9.00	0.3687	55.4	59.2	-6.96	**0.0435**	1333.1	1484.4	-11.35	0.767	62.8	64.6	-2.88	0.3644
18	F	636.4	514.0	19.24	**0.0482**	42.3	44.2	-4.38	**0.0496**	883.2	592.9	32.88	**0.021**	40.6	39.6	2.51	0.2762
19	F	1759.1	753.6	57.16	**0.0466**	78.0	81.0	-3.88	**0.0373**	1942.5	1075.6	44.63	0.0917	72.0	73.8	-2.57	0.2125
20	F	700.8	562.4	19.75	**0.0357**	59.2	62.9	-6.27	**0.0065**	803.6	666.6	17.05	0.0867	70.2	72.3	-3.06	0.0508
21	F	938.7	649.1	30.86	**0.0445**	53.8	55.0	-2.32	**0.0088**	932.5	704.8	24.42	**0.0487**	48.1	48.5	-0.86	0.3842
22	M	695.6	329.1	52.69	**0.0084**	70.1	71.6	-2.10	**0.0137**	396.8	1134.3	-185.88	**0.013**	71.8	71.5	0.34	0.8056
23	M	1792.8	885.9	50.59	**0.0118**	46.9	48.5	-3.42	**0.0225**	1902.6	1000.4	47.42	**0.0074**	47.4	48.2	-1.58	0.4843
24	M	370.4	297.5	19.67	**0.0354**	36.9	36.1	2.25	**0.0433**	365.2	352.6	3.43	0.7238	31.9	30.8	3.45	0.1135
25	F	418.0	538.4	-28.81	**0.0394**	40.7	42.7	-5.05	**0.0126**	356.8	450.7	-26.33	**0.0485**	51.9	50.4	2.82	0.1499
26	M	1403.7	820.2	41.56	**0.0023**	57.1	61.3	-7.36	**0.0404**	1147.0	1790.9	-56.14	0.2273	59.6	59.6	0.08	0.9718
27	M	1499.3	372.3	75.17	**0.0288**	59.0	61.0	-3.48	**0.036**	1173.8	836.5	28.73	0.1327	58.3	58.5	-0.23	0.8814
28	M	1543.9	764.5	50.49	**0.0484**	51.6	54.5	-5.63	**0.0434**	843.0	730.0	13.40	**0.0108**	60.2	62.1	-3.10	0.2687

Table 3

EEG Electrode Position	**Average ERD** (mean ± SD)	**Brain artery**	**Percentage changes in flow velocity** (mean ± SD)
C3	33.68 ± 25.03	LMCA	4.55 ± 2.68
C4	7.88 ± 36.70	RMCA	0.78 ± 2.96

Table 4

EEG Electrode Position	**Average ERD** (mean ± SD)		**Brain artery**	**Percentage changes in flow velocity** (mean ± SD)	
	Male	Female		Male	Female
C3	30.22 ± 23.41	30.81 ± 23.61	LMCA	4.33 ± 1.68	4.53 ± 2.18
C4	4.41 ± 36.70	11.62 ± 1.25	RMCA	0.44 ± 2.35	1.26 ± 1.91

Supplementary table 1

Gender	LMCA Depth	LMCA Gate	LMCA Gain	LMCA Ampl	RMCA Depth	RMCA Gate	RMCA Gain	RMCA Ampl
M	52	20	22	19%	52	20	22	19%
M	55	20	23	22%	55	20	23	19%
F	52	20	22	19%	52	20	22	19%
F	52	20	20	19%	52	20	20	19%
F	53	20	22	19%	58	20	22	19%
M	52	20	22	19%	52	20	22	19%
M	52	20	22	19%	52	20	22	19%
F	51	20	22	19%	54	20	20	19%
M	56	20	22	19%	60	20	22	19%
M	37	20	21	9%	55	20	22	19%
M	54	20	22	19%	52	20	22	19%
M	53	20	22	19%	52	20	22	19%
F	53	20	22	19%	53	20	21	19%
F	40	20	22	19%	42	20	21	19%
F	52	20	22	19%	52	20	22	19%
M	44	20	22	19%	40	20	22	19%
F	52	20	22	19%	52	20	22	19%
M	43	20	22	19%	51	20	22	19%
M	60	20	22	19%	52	20	22	19%
F	58	20	20	19%	53	20	20	19%
M	52	20	22	19%	52	20	22	19%
F	52	20	22	19%	52	20	22	19%
F	52	20	22	19%	57	20	24	19%
F	49	12	24	19%	49	12	22	19%
F	52	20	23	19%	51	20	23	19%
M	54	20	22	19%	61	20	22	19%
M	52	20	22	19%	52	20	22	19%
M	51	20	22	19%	47	20	22	19%

Figure 1

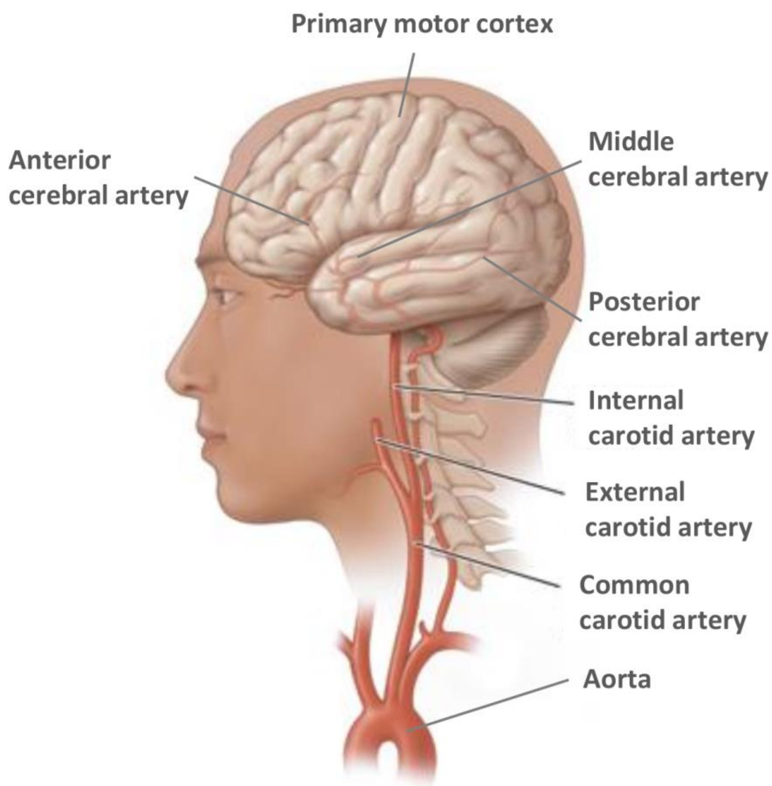
Primary motor cortex
Anterior cerebral artery
Middle cerebral artery
Posterior cerebral artery
Internal carotid artery
External carotid artery
Common carotid artery
Aorta

Figure 2

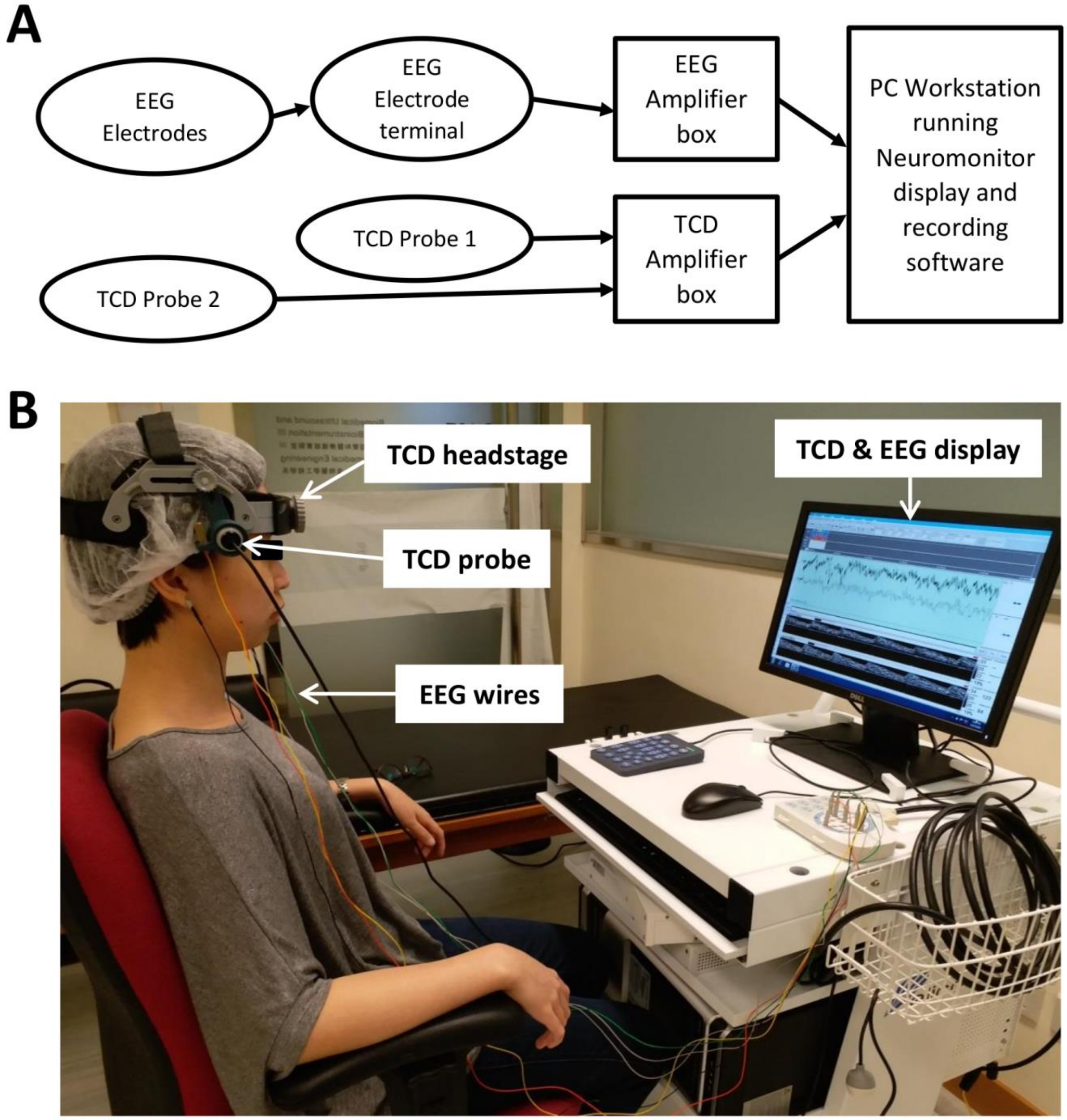
A
EEG Electrodes
EEG Electrode terminal
EEG Amplifier box
PC Workstation running Neuromonitor display and recording software
TCD Probe 1
TCD Probe 2
TCD Amplifier box
B
TCD headstage
TCD probe
EEG wires
TCD & EEG display

Figure 3

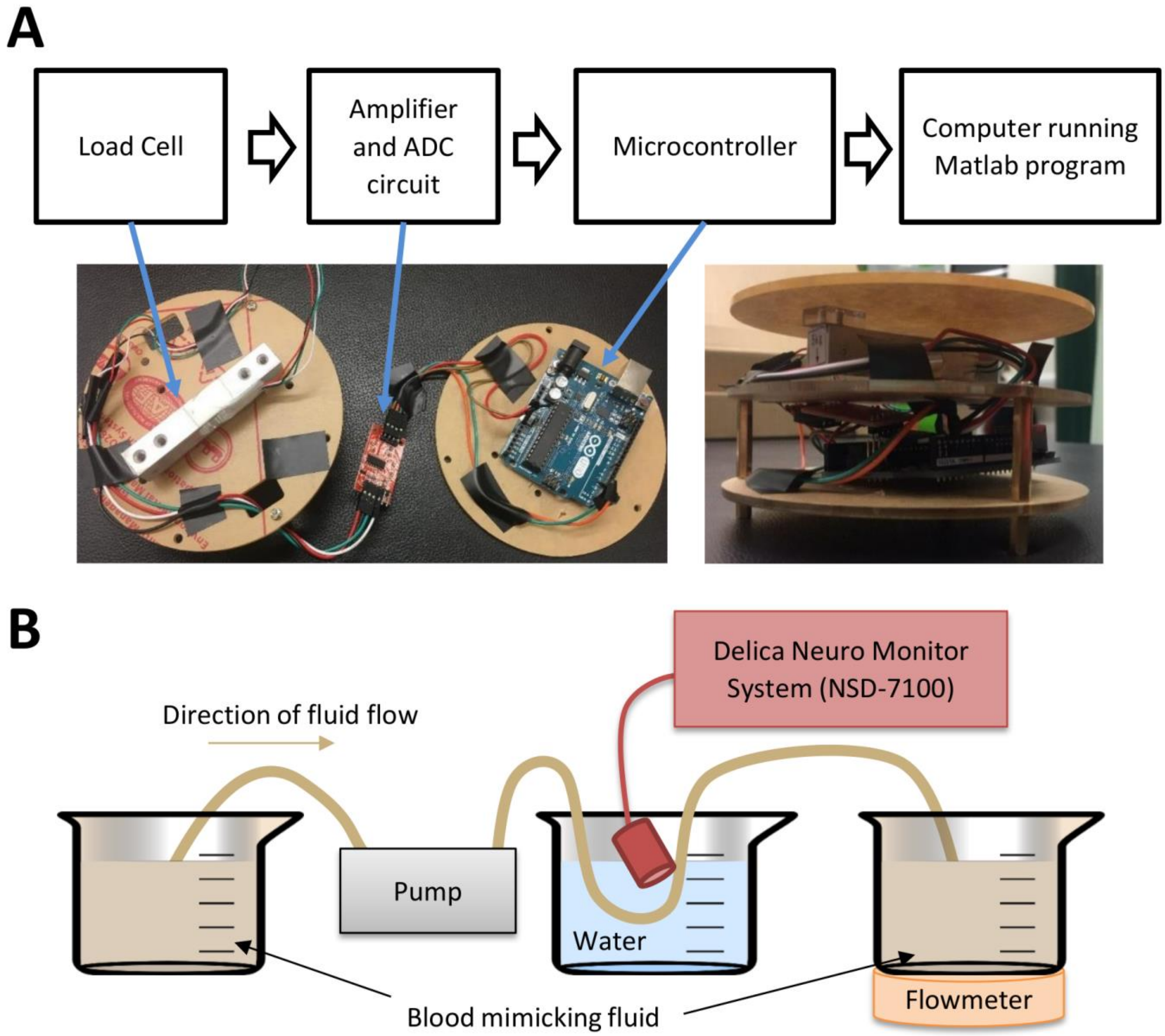
A
Load Cell
Amplifier and ADC circuit
Microcontroller
Computer running Matlab program
B
Delica Neuro Monitor System (NSD-7100)
Direction of fluid flow
Pump
Water
Blood mimicking fluid
Flowmeter

Figure 4

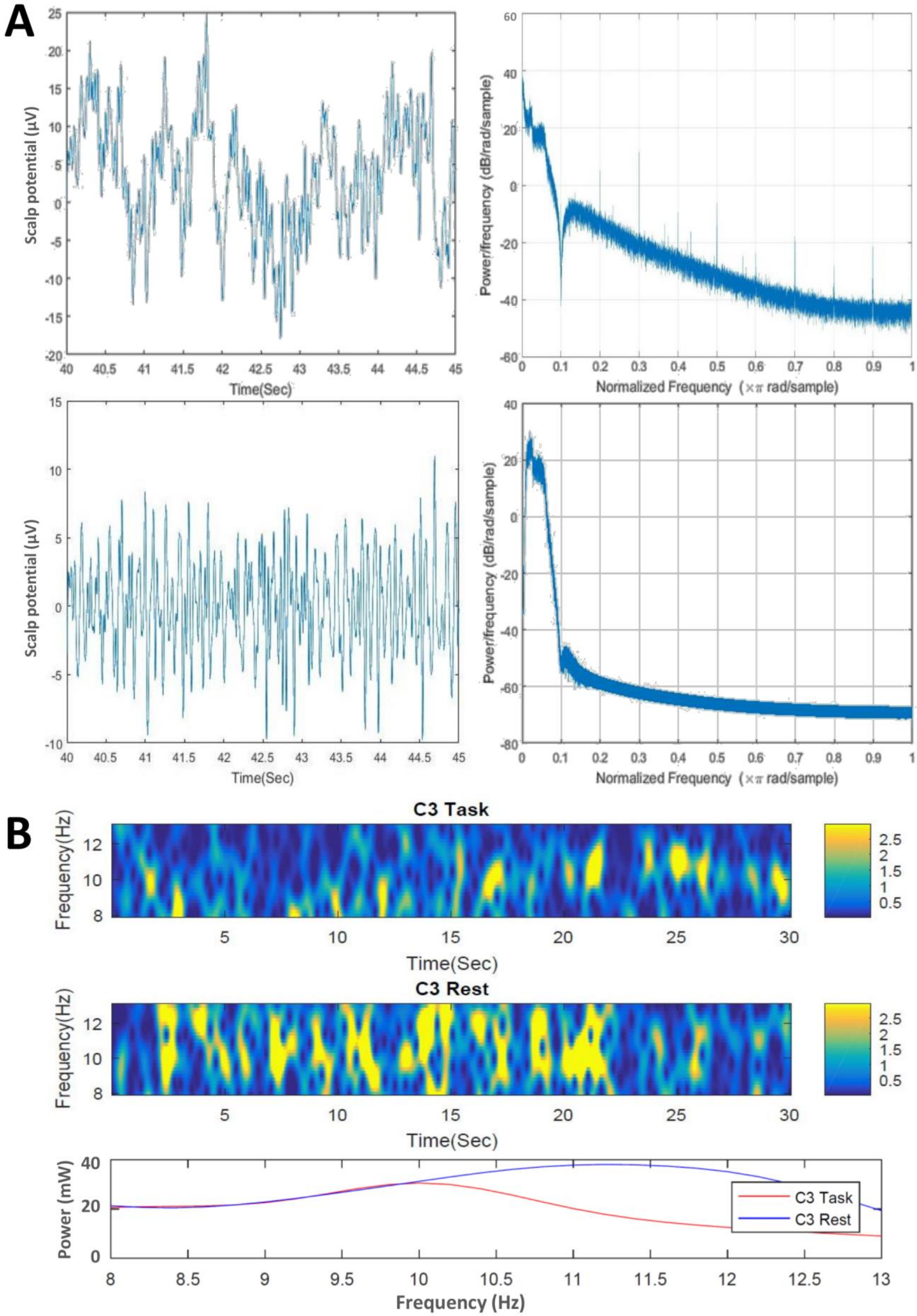

A
Scalp potential (µV)
Time(Sec)
Power/frequency (dB/rad/sample)
Normalized Frequency (×π rad/sample)
B
C3 Task
C3 Rest
Frequency(Hz)
Time(Sec)
Power (mW)
Frequency (Hz)
C3 Task
C3 Rest

Figure 5

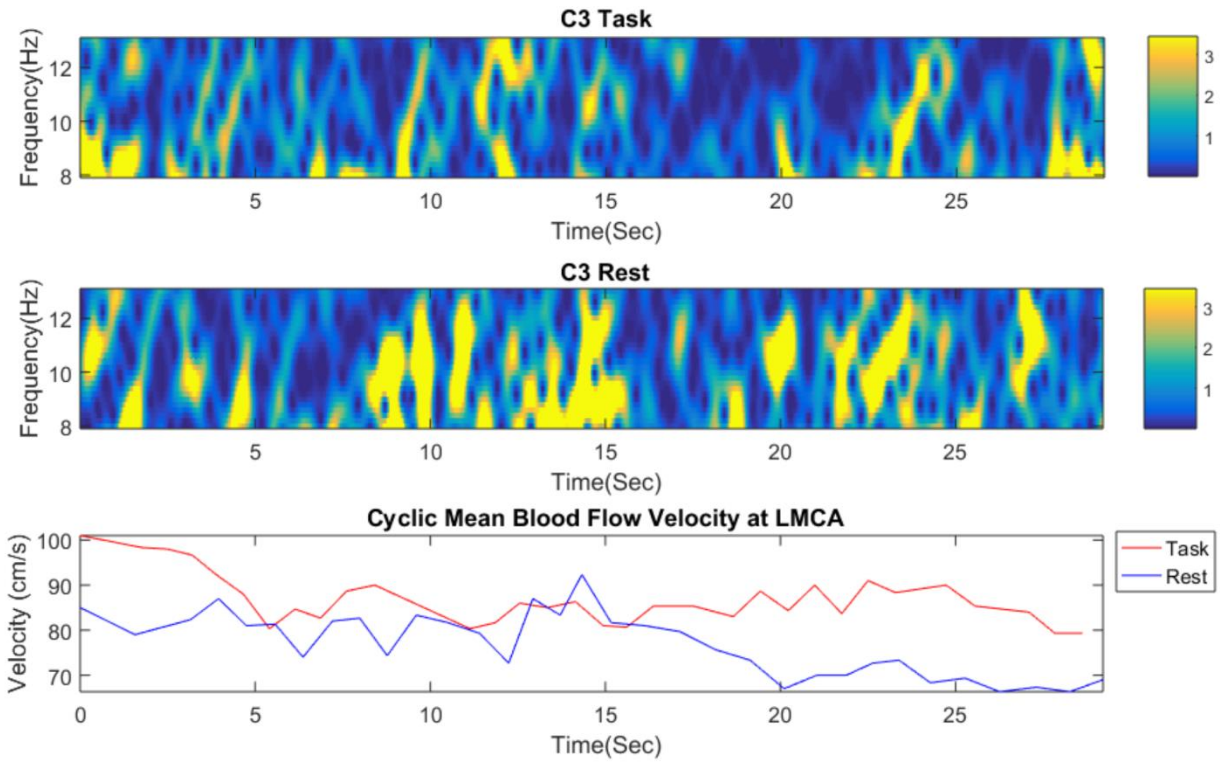
C3 Task
Frequency(Hz)
12
10
8
5
10
15
20
25
Time(Sec)
3
2
1
C3 Rest
Frequency(Hz)
12
10
8
5
10
15
20
25
Time(Sec)
3
2
1
Cyclic Mean Blood Flow Velocity at LMCA
Velocity (cm/s)
100
90
80
70
0
5
10
15
20
25
Time(Sec)
Task
Rest

Figure 6

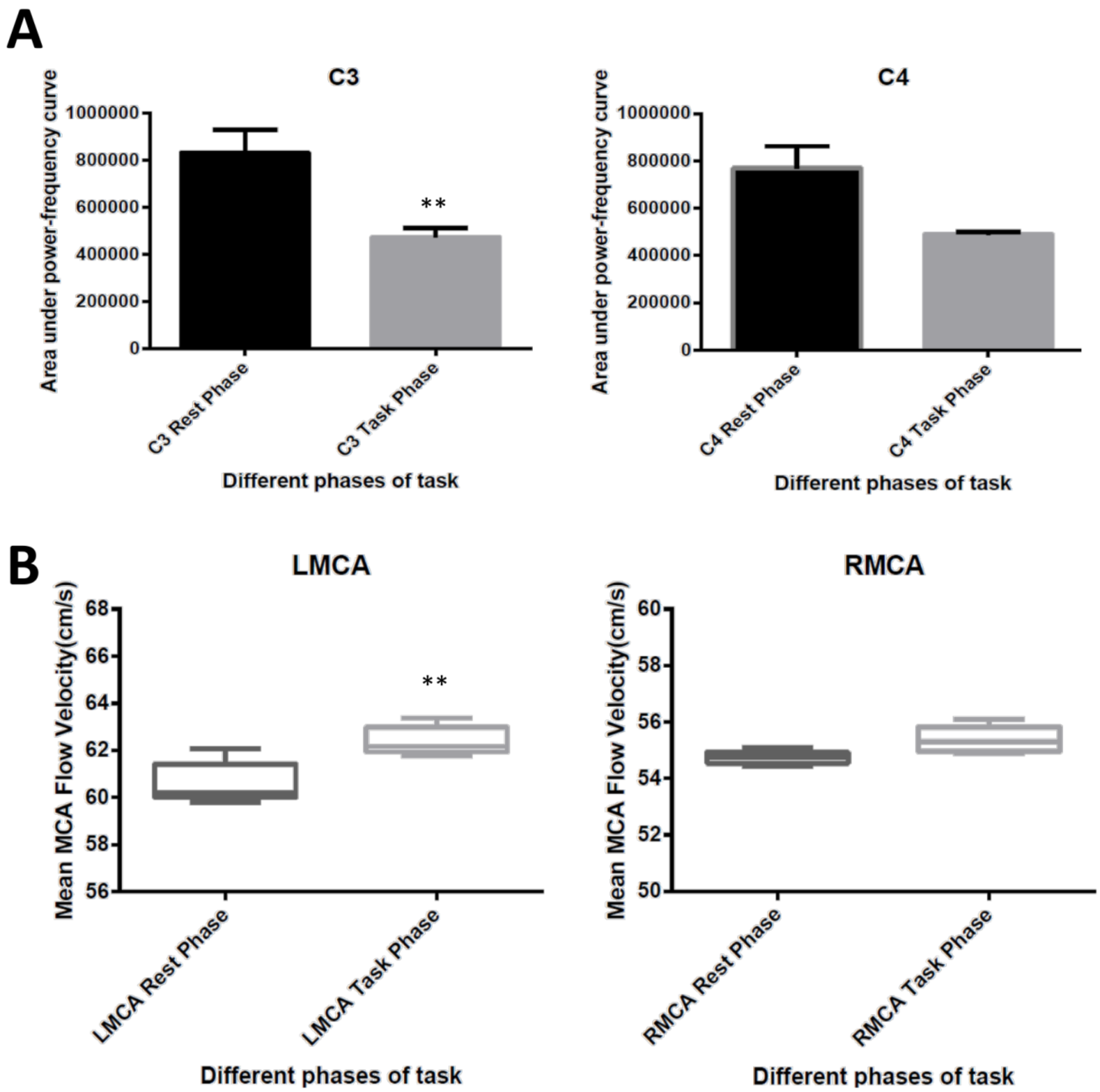
A
C3
Area under power-frequency curve
1000000
800000
600000
400000
200000
0
**
C3 Rest Phase
C3 Task Phase
Different phases of task
C4
Area under power-frequency curve
1000000
800000
600000
400000
200000
0
C4 Rest Phase
C4 Task Phase
Different phases of task
B
LMCA
Mean MCA Flow Velocity(cm/s)
68
66
64
62
60
58
56
**
LMCA Rest Phase
LMCA Task Phase
Different phases of task
RMCA
Mean MCA Flow Velocity(cm/s)
60
58
56
54
52
50
RMCA Rest Phase
RMCA Task Phase
Different phases of task

Figure 7

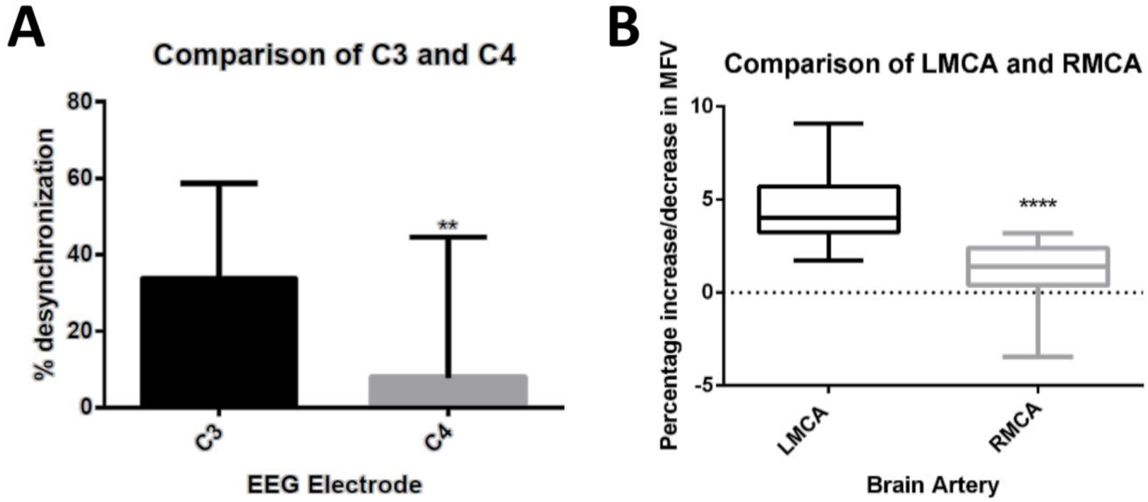
A
Comparison of C3 and C4
80
60
40
20
0
% desynchronization
**
C3
C4
EEG Electrode
B
Comparison of LMCA and RMCA
10
5
0
-5
Percentage increase/decrease in MFV
****
LMCA
RMCA
Brain Artery

Figure 8

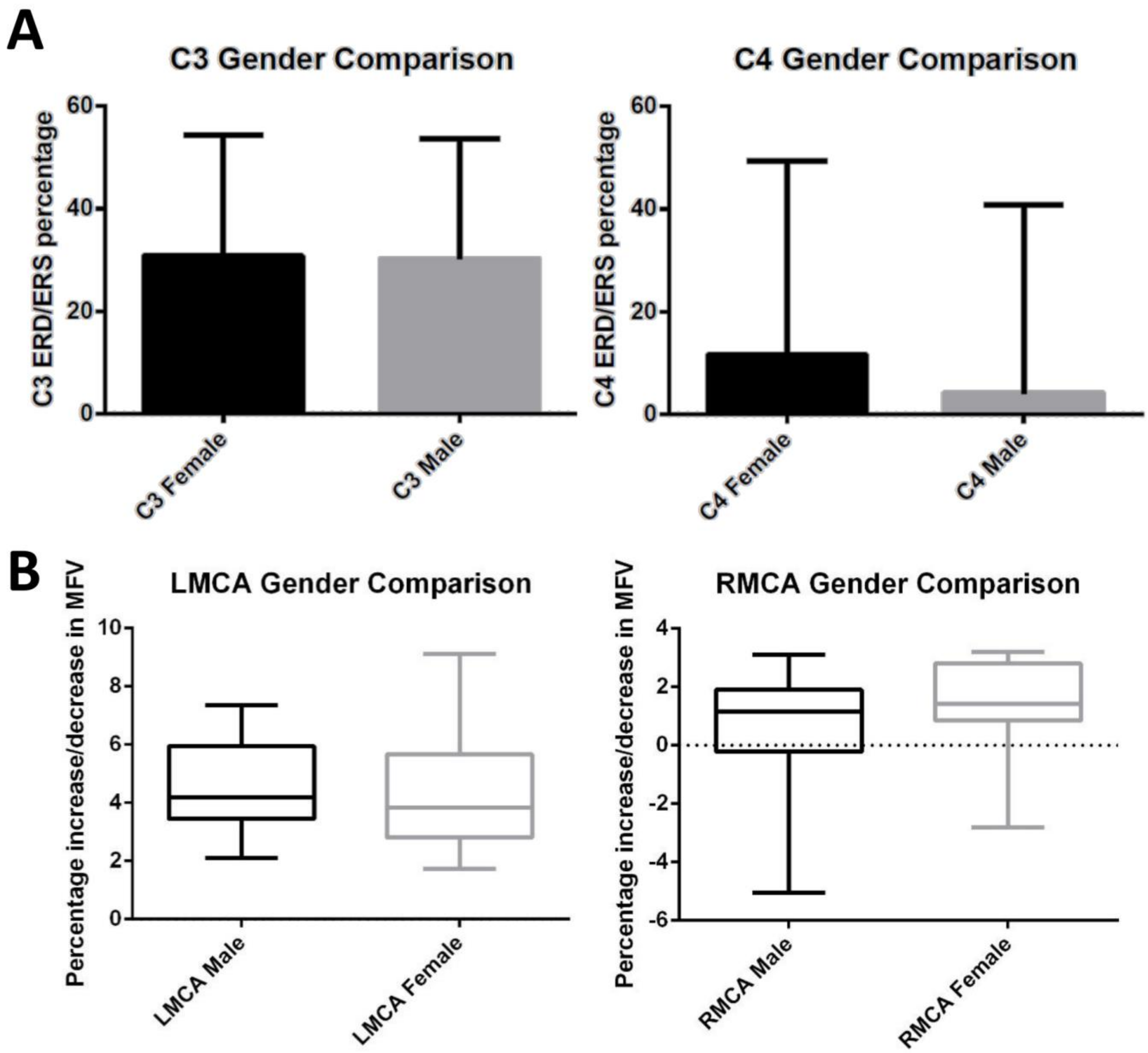
A
C3 Gender Comparison
C3 ERD/ERS percentage
60
40
20
0
C3 Female
C3 Male
C4 Gender Comparison
C4 ERD/ERS percentage
60
40
20
0
C4 Female
C4 Male
B
LMCA Gender Comparison
Percentage increase/decrease in MFV
10
8
6
4
2
0
LMCA Male
LMCA Female
RMCA Gender Comparison
Percentage increase/decrease in MFV
4
2
0
-2
-4
-6
RMCA Male
RMCA Female